

Electronic Supplementary Information (ESI)

Spontaneous symmetry breaking of Co(II) metal-organic frameworks from achiral precursors *via* asymmetrical crystallization

Ya-Dong Yu, Chan Luo, Bao-Yu Liu, Xiao-Chun Huang*, and Dan Li*

Department of Chemistry, Shantou University, Guangdong 515063, P. R. China

*E-mail: xchuang@stu.edu.cn

Table of Contents

S1	Experimental details
Fig. S2	ORTEP diagrams for MOFs 1P-NH₃ , 1M-NH₃ and 1P-H₂O
Fig. S3	Portion of the crystal structure of 1P-H₂O
Fig. S4	Topology analysis of 1M-NH₃ and 1P-H₂O
Table S1	Selected bond length and bond angles for MOFs 1P-NH₃ , 1M-NH₃ , and 1P-H₂O
Table S2-S3	Summary of multiple crystal data sets for zinc and cobalt CPs
Fig. S5	Solid state UV-Vis diffused reflectance spectra of 1M-NH₃ and 1P-H₂O
Fig. S6-S12	Solid state CD spectra for single crystals and bulk samples of racemic conglomerate 1P-NH₃ + 1M-NH₃ , 1P-H₂O and 1M-NH₃
Fig. S13	Curie plot of 1P-H₂O and 1M-NH₃
Fig. S14	PXRD patterns for 1P-NH₃ + 1M-NH₃ , 1P-H₂O and 1M-NH₃
Fig. S15	TGA plots for 1P-H₂O and 1M-NH₃
Fig. S16	CO ₂ sorption isotherm of 1P-H₂O
Fig. S17	Chiral GC results of the 2-butanol
Table S4	Chiral GC results of the 2-butanol

S1. Experimental Section

S1.1. Materials

The ligand 2H-imidazole-4-carboxylic acid (H_2L) was purchased from J&K Scientific Ltd. Metal salts, and organic solvents were commercially available and were used as received. The solvents used for synthesis were of analytical grade.

S1.2. Physical measurements

Infrared spectra were obtained as KBr disks on a Nicolet Avatar 360 FTIR spectrometer in the range of $4000\text{--}400\text{ cm}^{-1}$ (abbreviations used for the IR bands are w = weak, m = medium, b = broad, and vs = very strong). Elemental analyses (C, H, and N) were carried out with Elementar Vario EL Cube equipment. Thermogravimetric measurements were performed on a TA Instruments Q50 Thermogravimetric Analyzer under a nitrogen flow of $40\text{ mL}^{-1}\text{ min}$ at a typical heating rate of $10\text{ }^\circ\text{C min}^{-1}$. Powder X-ray diffraction (PXRD) experiments were performed on a D8 Advance X-ray diffractometer CuK α radiation. UV-vis diffused reflectance spectra were recorded with an Agilent 8453 UV-vis spectrophotometer (Agilent Technologies Co. Ltd.). Single crystal structures were determined using an Oxford Diffraction Gemini E instrument equipped with a graphite monochromator and ATLAS CCD detector (CrysAlis CCD, Oxford Diffraction Ltd.). The circular dichroism spectrum (CD) was recorded on a MOS 450 AF/CD device (Bio-Logic, Claix, France) spectropolarimeter with KCl pellets. Low pressure (up to 1 bar) gas adsorption isotherms of CO_2 were measured on the Micrometrics ASAP 2020 Surface Area and Porosity Analyzer. In one typical run, about 150 mg as-synthesis samples were activated at $180\text{ }^\circ\text{C}$ for 15 hours by using the "outgas" function of the surface area analyzer before measurements. Magnetic data were collected using crushed crystals of the sample on a Quantum Design MPMS XL-7 SQUID magnetometer. Chiral separation experiments were recorded by using gas chromatography (GC). Conditions Column: CHIRALDEX G-TA by ASTEC Company ($30\text{ m} \times 0.25\text{ mm I.D.}$). Column temperature: $26\text{ }^\circ\text{C}$. Carrier gas: $\text{N}_2\text{ }0.5\text{ mL/min}$, $\text{H}_2\text{ }0.5\text{ mL/min}$.

S1.3. X-ray crystallography

Summary of crystallographic data and details of data collection for **1P-NH₃**, **1M-NH₃** and **1P-H₂O** are given in **Table S1**. Single crystals with suitable dimensions were chosen under an optical microscope and mounted on a glass fiber for data collection. Intensity data for all crystals were collected using MoK α ($\lambda = 0.71073\text{ \AA}$) radiation on an Oxford Diffraction Gemini E instrument equipped with a graphite monochromator and ATLAS CCD detector under the room temperature (293 K). Structures were solved by direct methods (SHELXTL-97) and refined on F^2 using full-matrix least squares (SHELXTL-97).^[1,2] All non-hydrogen atoms were refined with anisotropic thermal parameters, and All non-hydrogen atoms were refined anisotropically till convergence is reached. Hydrogen atoms attached to the organic moieties present in all compounds are either located from the difference Fourier map or stereochemically fixed. After refining the coordination polymeric network in all three

compounds, some of the diffused peaks very close to each other with residual electron density ranging from 1.1\AA^{-3} to 1.9\AA^{-3} were observed in the difference Fourier map which can be attributed to disordered solvent molecules present in the crystal lattice. Attempts made to model these disordered peaks were unsuccessful since residual electron density of the peaks obtained was diffused and there was no obvious major site occupations for the solvent molecules. PLATON/SQUEEZE^[3] was used to correct the diffraction data for the contribution from disordered lattice solvent molecule. Final cycles of least-squares refinements improved the R-values with the modified data set after subtracting the contribution from the disordered solvent molecules using SQUEEZ program

S1.4. Synthesis of metal-organic frameworks

Synthesis of Conglomerate 1 (1P-NH₃ + 1M-NH₃):

The mixture Co(Ac)₂·4H₂O (0.4 mmol, 0.10 mg), H₂L (0.3 mmol, 0.034 g), and mixed solvents EtOH/THF/NH₃·H₂O (*v/v/v* = 4/1/1, 6 mL) were loaded into a 15-mL Teflon-lined reactor, stirred for 30 minutes at room temperature, then heated to 160 °C in a programmable oven for 72 h, followed by slow cooling (4 °C/h) to room temperature. After washing with ethanol, both irregular and triangular crystals with blackish-purple colors were obtained. Yield: 80% (based on ligand). IR (KBr pellet, cm⁻¹): 3400 (b), 1590 (s), 1550 (s), 1400 (s), 1230 (m), 1200 (w), 1100 (w), 830 (w), 800 (w), 670 (w). Elemental analysis (%) Calcd for ([Co₆(C₄H₂N₂O₂)₆(NH₃)·(H₂O)₆): C, 25.31; H, 2.37; N, 15.99. Found: C, 25.52; H, 2.20; N, 15.86.

Synthesis of 1M-NH₃

The mixture Co(Ac)₂·4H₂O (0.4 mmol, 0.10 mg), H₂L (0.3 mmol, 0.034 g), and mixed solvents CH₃CN/DMF/NH₃·H₂O (*v/v/v* = 4/1/1, 6 mL) were loaded into a 15-mL Teflon-lined reactor, stirred for 30 minutes at room temperature, then heated to 160 °C in a programmable oven for 72 h, followed by slow cooling (4 °C/h) to room temperature. After washing with ethanol, irregular crystals with blackish-purple colors were obtained. Yield: 85% (based on ligand). IR (KBr pellet, cm⁻¹): 3400 (b), 1590 (s), 1550 (s), 1400 (s), 1230 (m), 1200 (w), 1100 (w), 830 (w), 800 (w), 670 (w). Elemental analysis (%) Calcd for ([Co₆(C₄H₂N₂O₂)₆(NH₃)·(H₂O)₆): C, 25.31; H, 2.37; N, 15.99. Found: C, 25.22; H, 2.39; N, 16.12.

Synthesis of 1P-H₂O

The mixture Co(Ac)₂·4H₂O (0.4 mmol, 0.10 mg), H₂L (0.3 mmol, 0.034 g), and mixed solvents DMF/NH₃·H₂O (*v/v* = 4/1, 10 mL) were loaded into a 15-mL Teflon-lined reactor, stirred for 30 minutes at room temperature, then heated to 140 °C in a programmable oven for 72 h, followed by slow cooling (3 °C/h) to room temperature. After washing with ethanol, triangular crystals with reddish-purple colors were obtained. Yield: 55% (based on ligand). IR (KBr pellet, cm⁻¹): 3400 (b), 1590 (s), 1550 (s), 1400 (s), 1230 (m), 1200 (w), 1100 (w), 830 (w), 800 (w), 670 (w). Elemental analysis (%) Calcd for ([Co₆(C₄H₂N₂O₂)₆(H₂O)]·(H₂O)₆): C, 25.28; H, 2.28; N, 14.75. Found: C, 25.14; H, 2.45; N, 14.96.

Fig. S2 ORTEP diagrams for MOFs **1P-NH₃**, **1M-NH₃**, **1P-H₂O**

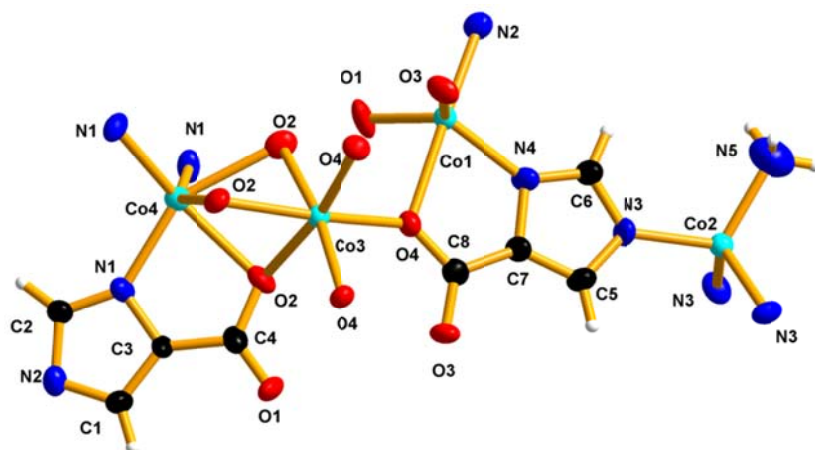


Fig. S2.1: ORTEP diagram depicting the coordination sphere with atom numbering scheme for **1P-NH₃** (50% probability factor for the thermal ellipsoids).

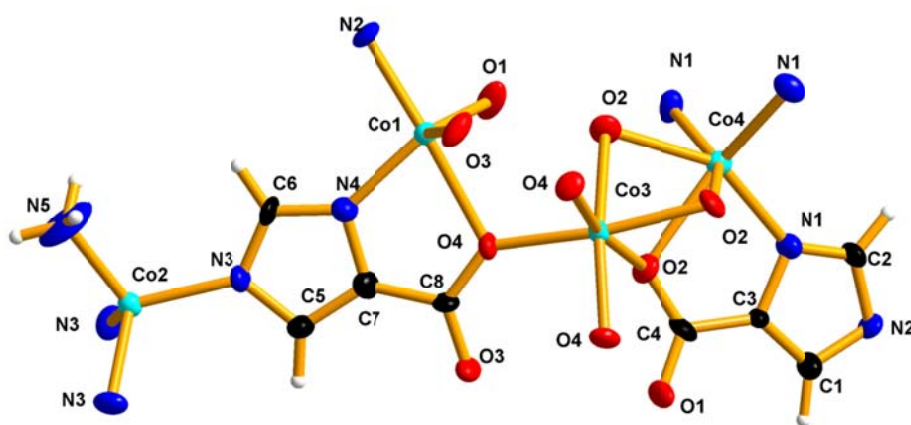


Fig. S2.2: ORTEP diagram depicting the coordination sphere with atom numbering scheme for **1M-NH₃** (50% probability factor for the thermal ellipsoids).

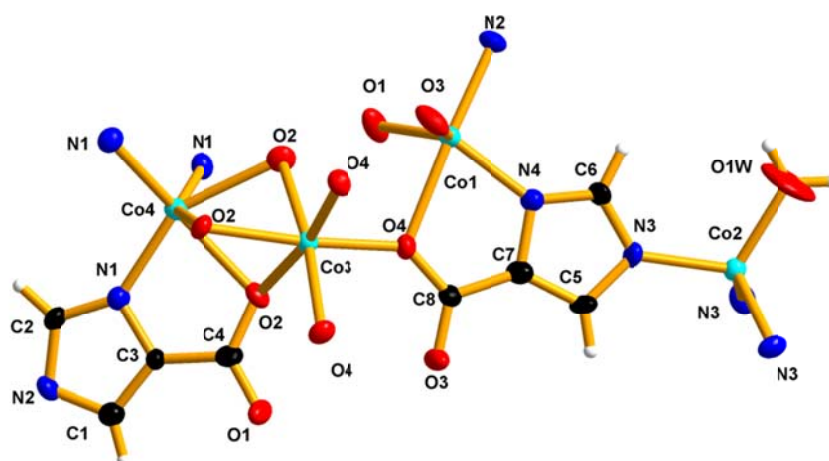


Fig. S2.3: ORTEP diagram depicting the coordination sphere with atom numbering scheme for **1P-H₂O** (50% probability factor for the thermal ellipsoids).

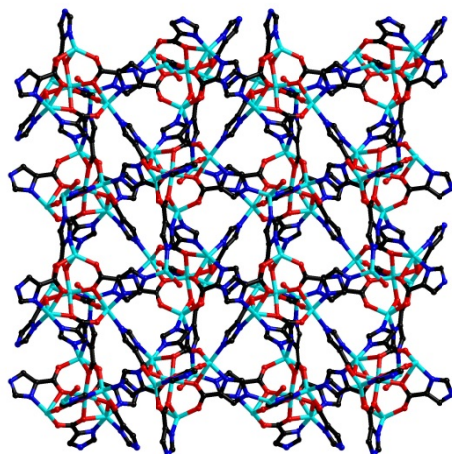


Fig. S3 Portion of the crystal structure of **1P-H₂O** as viewed along the *b*-axis. Turquoise, black, blue and red spheres represent Co, C, N and O atoms, respectively; H atoms have been omitted for clarity.

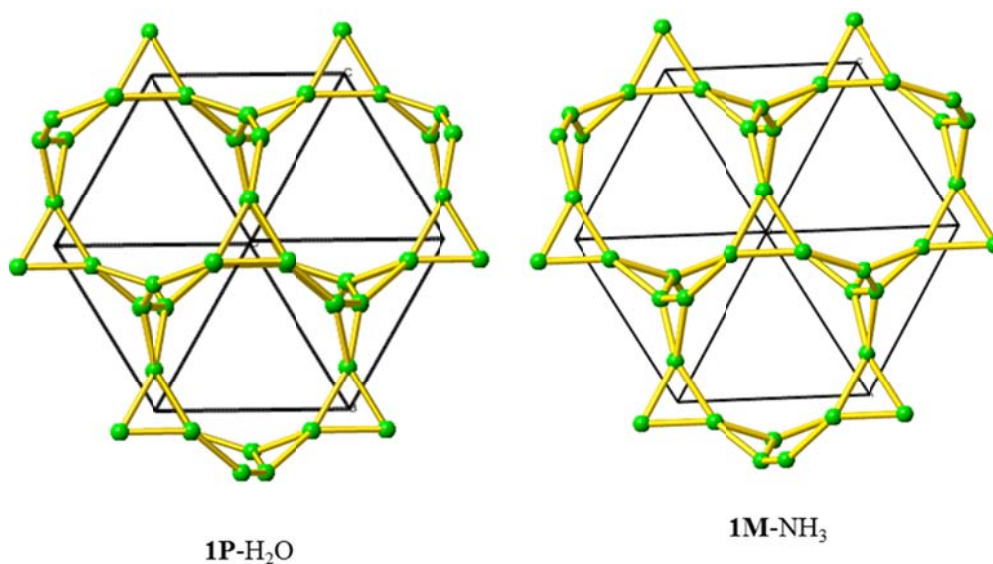


Figure S4. The underlying net **lcv** of **1P-H₂O** and **1M-NH₃** (the identification of the nets and computation of their ideal symmetry are performed through the program *Systre*.^[4] Note **lcv** is known to RSCR.^[5])

Table S1 Selected bond length and bond angle for MOFs **1P-NH₃**, **1M-NH₃** and **1P-H₂O**

1P-NH ₃			
Co(1)-O(1)#1	1.997(6)	Co(3)-O(4)#1	2.036(5)
Co(1)-O(3)#2	1.997(6)	Co(3)-O(2)	2.088(6)
Co(1)-N(4)	2.019(7)	Co(3)-O(2)#1	2.088(6)
Co(1)-N(2)#3	2.043(8)	Co(3)-O(2)#2	2.088(6)
Co(1)-O(4)	2.262(6)	Co(4)-N(1)	2.064(7)
Co(2)-N(5)	1.97(3)	Co(4)-N(1)#2	2.064(7)
Co(2)-N(3)	2.003(7)	Co(4)-N(1)#1	2.064(7)

Co(2)-N(3)#4	2.003(7)	Co(4)-O(2)#2	2.262(6)
Co(2)-N(3)#5	2.003(7)	Co(4)-O(2)#1	2.262(6)
Co(3)-O(4)#2	2.036(5)	Co(4)-O(2)	2.262(6)
Co(3)-O(4)	2.036(5)		
O(1)#1-Co(1)-O(3)#2	125.9(3)	O(4)-Co(3)-O(2)#1	92.3(2)
O(1)#1-Co(1)-N(4)	118.1(3)	O(4)#1-Co(3)-O(2)#1	170.5(3)
O(3)#2-Co(1)-N(4)	112.1(3)	O(2)-Co(3)-O(2)#1	78.5(3)
O(1)#1-Co(1)-N(2)#3	91.1(3)	O(4)#2-Co(3)-O(2)#2	170.5(3)
O(3)#2-Co(1)-N(2)#3	98.0(3)	O(4)-Co(3)-O(2)#2	97.3(2)
N(4)-Co(1)-N(2)#3	101.2(3)	O(4)#1-Co(3)-O(2)#2	92.3(2)
O(1)#1-Co(1)-O(4)	86.0(3)	O(2)-Co(3)-O(2)#2	78.5(3)
O(3)#2-Co(1)-O(4)	88.2(2)	O(2)#1-Co(3)-O(2)#2	78.5(3)
N(4)-Co(1)-O(4)	75.4(2)	N(1)-Co(4)-N(1)#2	106.7(2)
N(2)#3-Co(1)-O(4)	173.7(3)	N(1)-Co(4)-N(1)#1	106.7(2)
N(5)-Co(2)-N(3)	111.4(2)	N(1)#2-Co(4)-N(1)#1	106.7(2)
N(5)-Co(2)-N(3)#4	111.4(2)	N(1)-Co(4)-O(2)#2	149.0(3)
N(3)-Co(2)-N(3)#4	107.5(2)	N(1)#2-Co(4)-O(2)#2	77.6(3)
N(5)-Co(2)-N(3)#5	111.4(2)	N(1)#1-Co(4)-O(2)#2	101.1(3)
N(3)-Co(2)-N(3)#5	107.5(2)	N(1)-Co(4)-O(2)#1	101.1(3)
N(3)#4-Co(2)-N(3)#5	107.5(2)	N(1)#2-Co(4)-O(2)#1	149.0(3)
O(4)#2-Co(3)-O(4)	91.4(3)	N(1)#1-Co(4)-O(2)#1	77.6(3)
O(4)#2-Co(3)-O(4)#1	91.4(3)	O(2)#2-Co(4)-O(2)#1	71.5(2)
O(4)-Co(3)-O(4)#1	91.4(3)	N(1)-Co(4)-O(2)	77.6(3)
O(4)#2-Co(3)-O(2)	92.3(2)	N(1)#2-Co(4)-O(2)	101.1(3)
O(4)-Co(3)-O(2)	170.5(3)	N(1)#1-Co(4)-O(2)	149.0(3)
O(4)#1-Co(3)-O(2)	97.3(2)	O(2)#2-Co(4)-O(2)	71.5(2)
O(4)#2-Co(3)-O(2)#1	97.3(2)	O(2)#1-Co(4)-O(2)	71.5(2)
Symmetry transformations: #1 -z-1,x-1/2,-y-3/2; #2 y+1/2,-z-3/2,-x-1; #3 x+1/2,-y-3/2,-z-2; #4 -z-1/2,-x,y-1/2; #5 -y,z+1/2,-x-1/2			
1M-NH₃			
Co(1)-O(3)	1.987(3)	Co(3)-O(4)#2	2.041(3)
Co(1)-O(1)#1	2.011(3)	Co(3)-O(2)#6	2.099(3)
Co(1)-N(4)#2	2.016(4)	Co(3)-O(2)#7	2.099(3)
Co(1)-N(2)	2.038(4)	Co(3)-O(2)#1	2.099(3)
Co(1)-O(4)#2	2.273(3)	Co(4)-N(1)#3	2.063(4)
Co(2)-N(5)	1.947(16)	Co(4)-N(1)	2.063(4)
Co(2)-N(3)#3	2.018(4)	Co(4)-N(1)#4	2.063(4)
Co(2)-N(3)	2.018(4)	Co(4)-O(2)	2.273(4)
Co(2)-N(3)#4	2.018(4)	Co(4)-O(2)#4	2.273(3)
Co(3)-O(4)#5	2.041(3)	Co(4)-O(2)#3	2.273(4)
Co(3)-O(4)	2.041(3)		
O(3)-Co(1)-O(1)#1	125.10(16)	O(4)-Co(3)-O(2)#7	170.32(14)
O(3)-Co(1)-N(4)#2	112.85(18)	O(4)#2-Co(3)-O(2)#7	96.81(13)
O(1)#1-Co(1)-N(4)#2	118.02(18)	O(2)#6-Co(3)-O(2)#7	78.88(15)

O(3)-Co(1)-N(2)	98.26(16)	O(4)#5-Co(3)-O(2)#1	170.32(14)
O(1)#1-Co(1)-N(2)	91.43(16)	O(4)-Co(3)-O(2)#1	96.81(13)
N(4)#2-Co(1)-N(2)	100.87(17)	O(4)#2-Co(3)-O(2)#1	91.83(14)
O(3)-Co(1)-O(4)#2	88.68(13)	O(2)#6-Co(3)-O(2)#1	78.88(15)
O(1)#1-Co(1)-O(4)#2	85.34(14)	O(2)#7-Co(3)-O(2)#1	78.88(15)
N(4)#2-Co(1)-O(4)#2	75.31(14)	N(1)#3-Co(4)-N(1)	107.00(12)
N(2)-Co(1)-O(4)#2	172.98(15)	N(1)#3-Co(4)-N(1)#4	107.00(12)
N(5)-Co(2)-N(3)#3	111.05(13)	N(1)-Co(4)-N(1)#4	107.00(12)
N(5)-Co(2)-N(3)	111.05(12)	N(1)#3-Co(4)-O(2)	149.13(15)
N(3)#3-Co(2)-N(3)	107.84(13)	N(1)-Co(4)-O(2)	77.36(14)
N(5)-Co(2)-N(3)#4	111.05(13)	N(1)#4-Co(4)-O(2)	100.46(15)
N(3)#3-Co(2)-N(3)#4	107.84(13)	N(1)#3-Co(4)-O(2)#4	100.46(15)
N(3)-Co(2)-N(3)#4	107.84(13)	N(1)-Co(4)-O(2)#4	149.13(14)
O(4)#5-Co(3)-O(4)	91.96(14)	N(1)#4-Co(4)-O(2)#4	77.36(14)
O(4)#5-Co(3)-O(4)#2	91.96(14)	O(2)-Co(4)-O(2)#4	71.83(13)
O(4)-Co(3)-O(4)#2	91.96(14)	N(1)#3-Co(4)-O(2)#3	77.36(14)
O(4)#5-Co(3)-O(2)#6	96.81(13)	N(1)-Co(4)-O(2)#3	100.46(15)
O(4)-Co(3)-O(2)#6	91.83(14)	N(1)#4-Co(4)-O(2)#3	149.13(14)
O(4)#2-Co(3)-O(2)#6	170.32(14)	O(2)-Co(4)-O(2)#3	71.83(13)
O(4)#5-Co(3)-O(2)#7	91.83(14)	O(2)#4-Co(4)-O(2)#3	71.83(13)

Symmetry transformations: #1 -z,x+1/2,-y+1/2; #2 z-1,x+1,y; #3 -z+1/2,-x,y+1/2; #4 -y,z-1/2,-x+1/2; #5 y-1,z,x+1; #6 x-1/2,-y+1/2,-z+1; #7 -y-1/2,-z+1,x+1/2

1P-H₂O

Co(1)-O(3)#1	1.989(3)	Co(3)-O(4)#5	2.041(3)
Co(1)-O(1)#1	2.010(3)	Co(3)-O(2)#1	2.097(3)
Co(1)-N(4)	2.025(4)	Co(3)-O(2)#5	2.097(3)
Co(1)-N(2)#2	2.042(4)	Co(3)-O(2)	2.097(3)
Co(1)-O(4)	2.278(3)	Co(4)-N(1)#5	2.057(4)
Co(2)-O(1W)	1.983(15)	Co(4)-N(1)#1	2.057(4)
Co(2)-N(3)	2.015(4)	Co(4)-N(1)	2.057(4)
Co(2)-N(3)#3	2.015(4)	Co(4)-O(2)	2.267(3)
Co(2)-N(3)#4	2.015(4)	Co(4)-O(2)#5	2.267(3)
Co(3)-O(4)#1	2.041(3)	Co(4)-O(2)#1	2.267(3)
Co(3)-O(4)	2.041(3)		
O(3)#1-Co(1)-O(1)#1	123.76(16)	O(4)-Co(3)-O(2)#5	170.20(14)
O(3)#1-Co(1)-N(4)	113.25(17)	O(4)#5-Co(3)-O(2)#5	96.93(12)
O(1)#1-Co(1)-N(4)	119.05(17)	O(2)#1-Co(3)-O(2)#5	78.80(14)
O(3)#1-Co(1)-N(2)#2	98.45(15)	O(4)#1-Co(3)-O(2)	170.20(14)
O(1)#1-Co(1)-N(2)#2	91.44(15)	O(4)-Co(3)-O(2)	96.93(12)
N(4)-Co(1)-N(2)#2	100.38(16)	O(4)#5-Co(3)-O(2)	91.76(13)
O(3)#1-Co(1)-O(4)	88.52(13)	O(2)#1-Co(3)-O(2)	78.80(14)
O(1)#1-Co(1)-O(4)	85.85(13)	O(2)#5-Co(3)-O(2)	78.80(14)
N(4)-Co(1)-O(4)	75.33(13)	N(1)#5-Co(4)-N(1)#1	107.29(12)
N(2)#2-Co(1)-O(4)	172.88(14)	N(1)#5-Co(4)-N(1)	107.29(12)

O(1W)-Co(2)-N(3)	110.38(12)	N(1)#1-Co(4)-N(1)	107.29(12)
O(1W)-Co(2)-N(3)#3	110.38(12)	N(1)#5-Co(4)-O(2)	149.11(14)
N(3)-Co(2)-N(3)#3	108.55(12)	N(1)#1-Co(4)-O(2)	99.98(14)
O(1W)-Co(2)-N(3)#4	110.38(12)	N(1)-Co(4)-O(2)	77.25(13)
N(3)-Co(2)-N(3)#4	108.55(12)	N(1)#5-Co(4)-O(2)#5	77.25(13)
N(3)#3-Co(2)-N(3)#4	108.55(12)	N(1)#1-Co(4)-O(2)#5	149.11(14)
O(4)#1-Co(3)-O(4)	91.99(13)	N(1)-Co(4)-O(2)#5	99.98(14)
O(4)#1-Co(3)-O(4)#5	91.99(13)	O(2)-Co(4)-O(2)#5	71.90(12)
O(4)-Co(3)-O(4)#5	91.99(13)	N(1)#5-Co(4)-O(2)#1	99.99(14)
O(4)#1-Co(3)-O(2)#1	96.93(12)	N(1)#1-Co(4)-O(2)#1	77.25(13)
O(4)-Co(3)-O(2)#1	91.76(13)	N(1)-Co(4)-O(2)#1	149.11(14)
O(4)#5-Co(3)-O(2)#1	170.20(14)	O(2)-Co(4)-O(2)#1	71.90(12)
O(4)#1-Co(3)-O(2)#5	91.76(13)	O(2)#5-Co(4)-O(2)#1	71.90(12)

Symmetry transformations: #1 -z-1,x-1/2,-y-3/2; #2 -y-1/2,-z-2,x-1/2; #3 z+1/2,-x-3/2,-y-2; #4 -y-3/2,-z-2,x-1/2; #5 y+1/2,-z-3/2,-x-1

Table S2 A summary of structure determinations of ten randomly selected reddish-purple and triangular crystals of **1P**-H₂O: Cell parameters, *R* factors, Flack absolute structure parameters for each refinement in *P*2₁3 space group and observed helicity are given.

SN	a	Vol.	<i>R</i> 1	<i>wR</i> 2	Flack parameter	Helicity
1	17.465(2)	5326.9(12)	0.0538	0.1545	0.98(4)	M
2	17.49820(10)	5357.72(5)	0.0394	0.1436	0.03(3)	P
3	17.5204(2)	5378.14(11)	0.0656	0.1964	0.04(6)	P
4	17.4524(8)	5315.8(4)	0.0549	0.1618	0.00(5)	P
5	17.5332(5)	5389.9(3)	0.0509	0.1755	0.03(4)	P
6	17.43180(10)	5296.96(5)	0.0657	0.1952	-0.011(10)	P
7	17.4907(2)	5350.83(11)	0.0656	0.2045	-0.03(5)	P
8	17.45850(10)	5321.34(5)	0.0581	0.1828	0.01(4)	P
9	17.46890(10)	5330.85(5)	0.0583	0.1861	0.03(4)	P
10	17.46840(10)	5330.40(5)	0.0441	0.1308	0.01(3)	P

Table S3 A summary of structure determinations of ten randomly selected blackish-purple and irregular crystals of **1M-NH₃**: Cell parameters, *R* factors, Flack absolute structure parameters for each refinement in *P*2₁3 space group and observed helicity are given.

SN	a	Vol.	<i>R</i> 1	<i>wR</i> 2	Flack parameter	Helicity
1	17.47050(10)	5332.32(5)	0.0418	0.1457	0.00(4)	M
2	17.46870(10)	5330.67(5)	0.0449	0.1453	0.02(4)	M
3	17.50350(10)	5362.59(5)	0.0395	0.1323	0.00(3)	M
4	17.4779(3)	5339.10(16)	0.0770	0.1688	0.94(7)	P
5	17.50570(10)	5364.61(5)	0.0490	0.1521	0.01(3)	M
6	17.51450(10)	5372.71(5)	0.0531	0.1704	-0.05(4)	M
7	17.51760(10)	5375.56(5)	0.0561	0.1873	-0.07(4)	M
8	17.48820(10)	5348.54(5)	0.0520	0.1733	0.03(4)	M
9	17.48450(10)	5345.15(5)	0.0550	0.1824	0.05(4)	M
10	17.50280(10)	5361.95(5)	0.0491	0.1669	0.00(4)	M

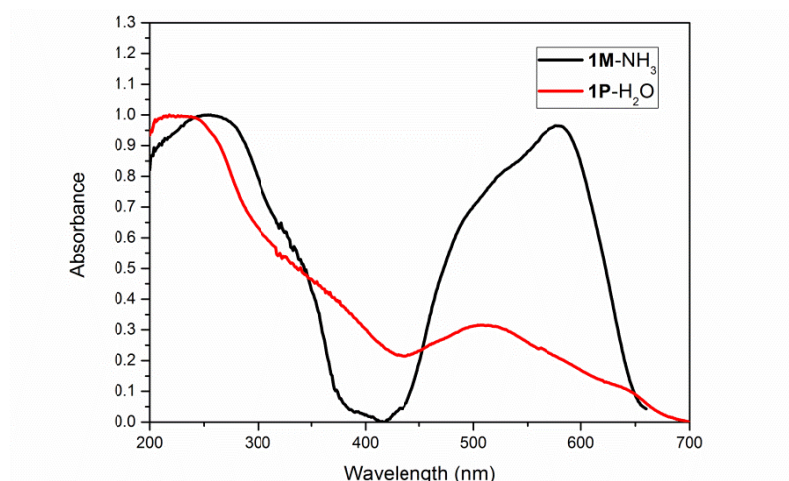


Fig. S5 Solid state UV-vis diffused reflectance spectra of **1M-NH₃** and **1P-H₂O** (using BaSO₄ as substrate).

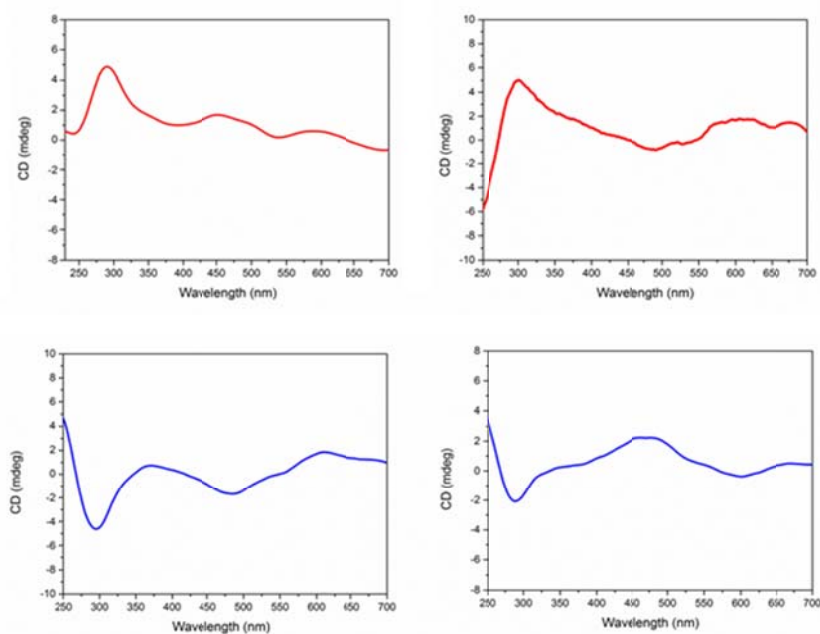


Fig. S6 Solid state CD spectra recorded for four blackish-purple and triangular single crystals of racemic conglomerate (**1P-NH₃** + **1M-NH₃**). Two of them show positive dichroic signal approximately at 300 nm (top), the other two show the opposite signals (bottom).

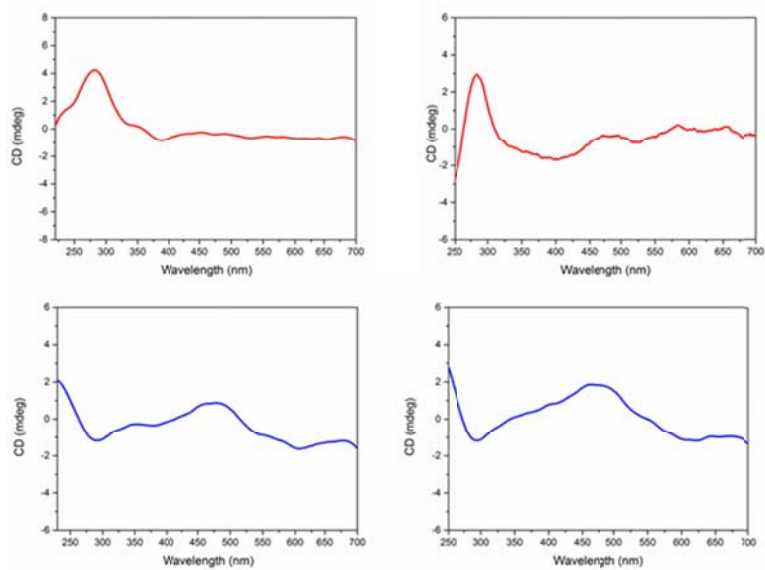


Fig. S7 Solid state CD spectra recorded for four blackish-purple and irregular single crystals of racemic conglomerate (**1P-NH₃** + **1M-NH₃**). Two of them show positive dichroic signal approximately at 300 nm (top), the other two shows the opposite signal (bottom)

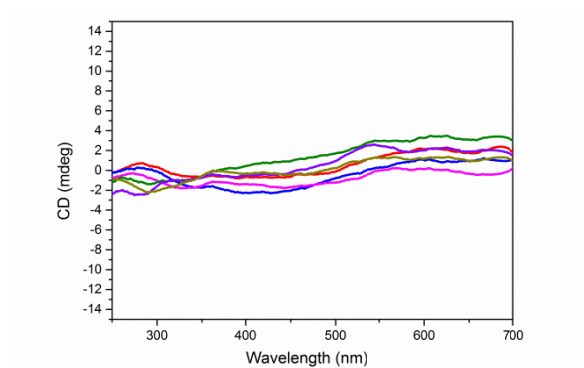


Fig. S8 Solid state CD spectra of bulk samples of **1** (containing both **1P-NH₃** and **1M-NH₃**) from six batches. All of them are almost CD silent, which show the formation of racemic conglomerate.

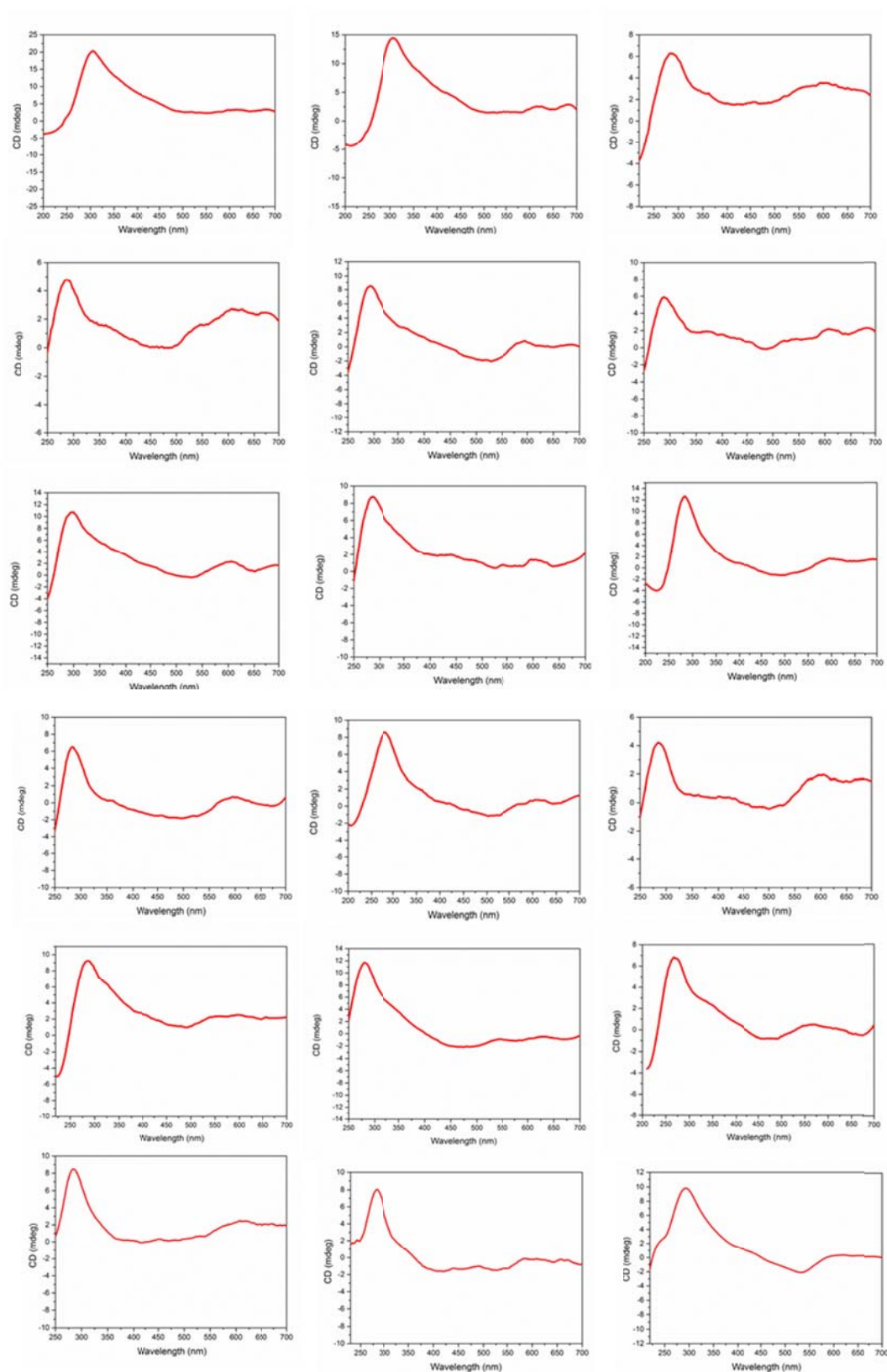


Fig. S9 Solid state CD spectra of bulk samples of **1P**-H₂O from eighteen batches. Positive dichroic signal approximately at 300 nm for all samples indicate the bulk homochirality nature of **1P**-H₂O.

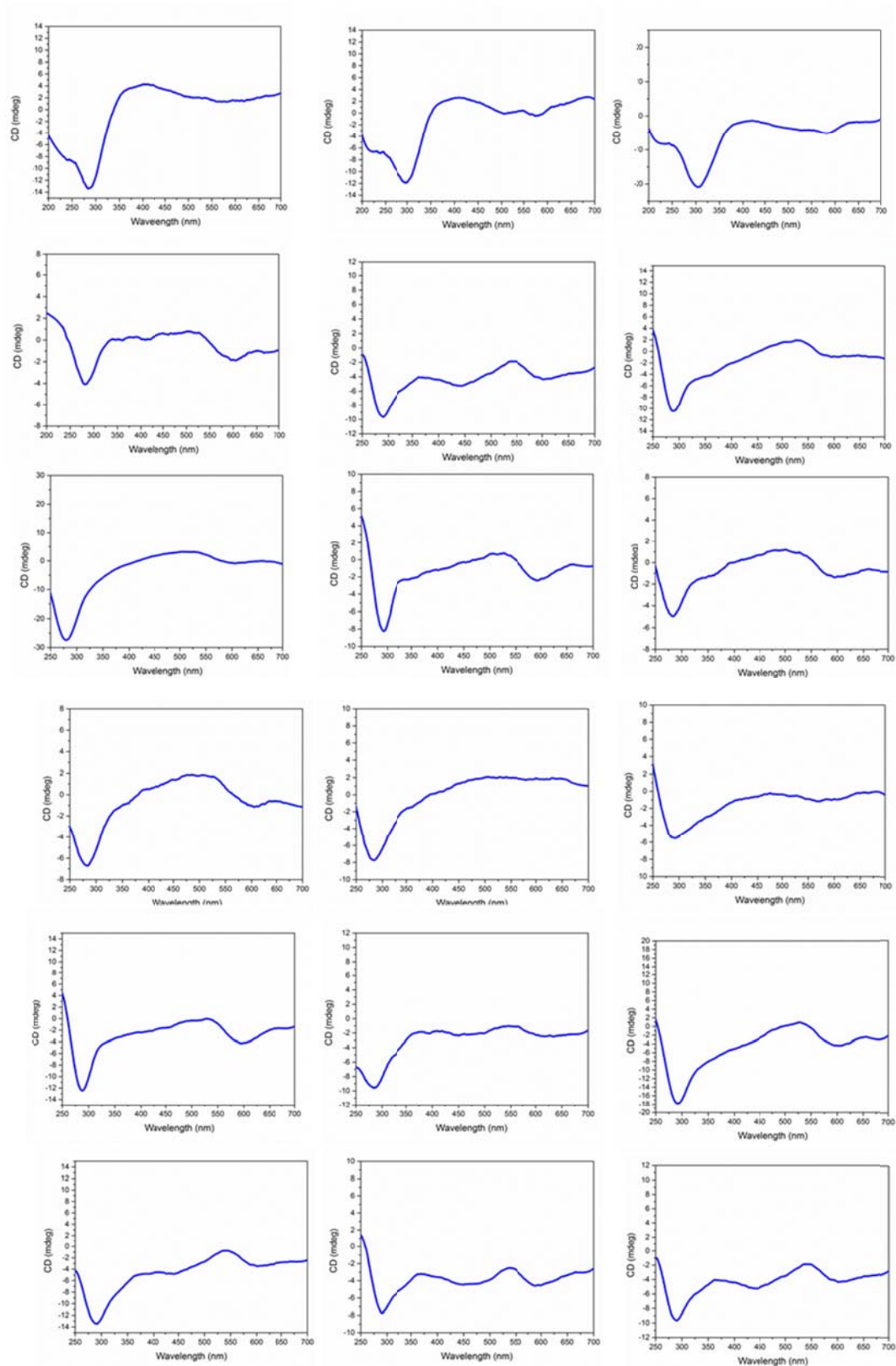


Fig. S10 Solid state CD spectra of bulk samples of **1M-H₂O** from eighteen batches. Negative dichroic signal approximately at 300 nm for all samples indicate the bulk homochirality nature of **1M-H₂O**.

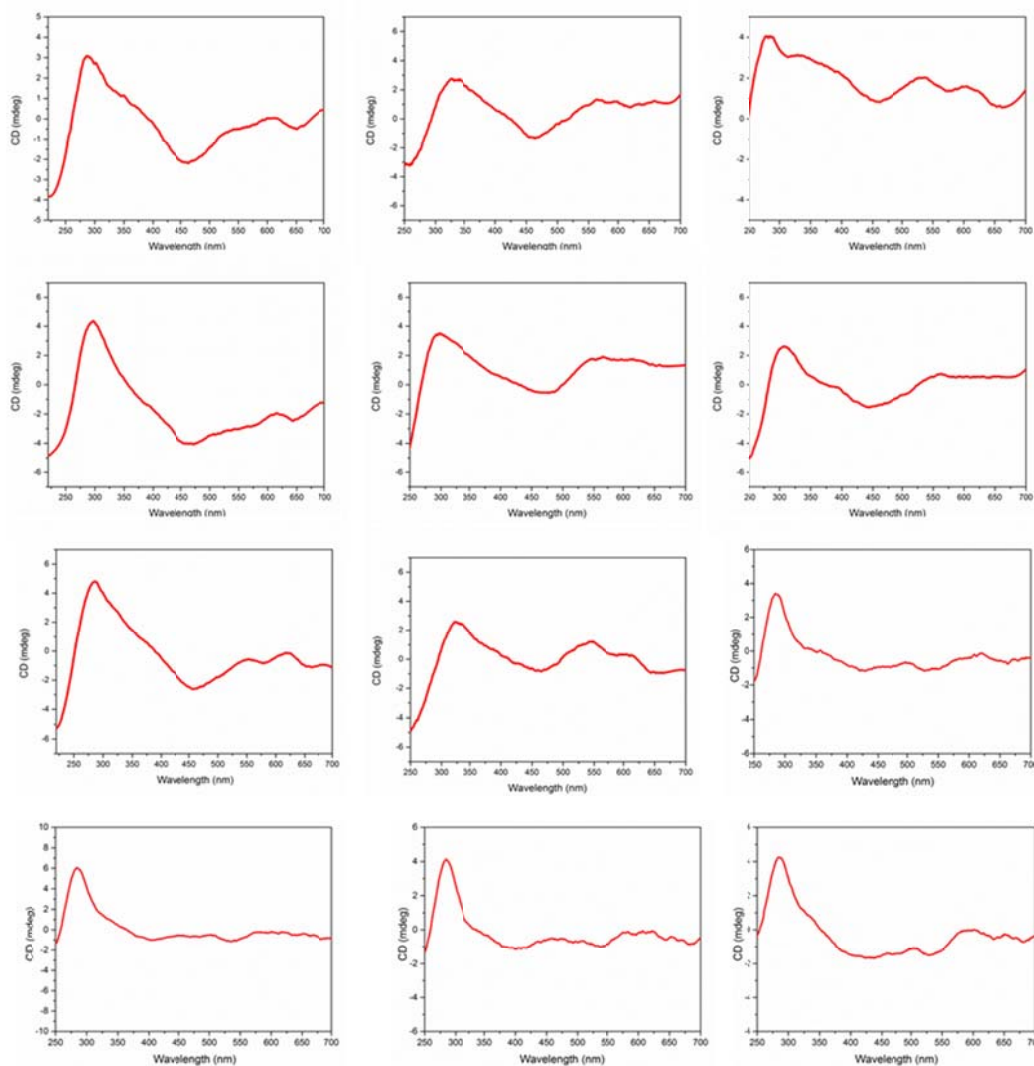


Fig. S11 Solid state CD spectra recorded for twelve reddish-purple and triangular single crystals of **1P**-H₂O. Positive dichroic signal approximately at 300 nm for all samples indicate the exclusive formation of enantiomorph **1P**-H₂O.

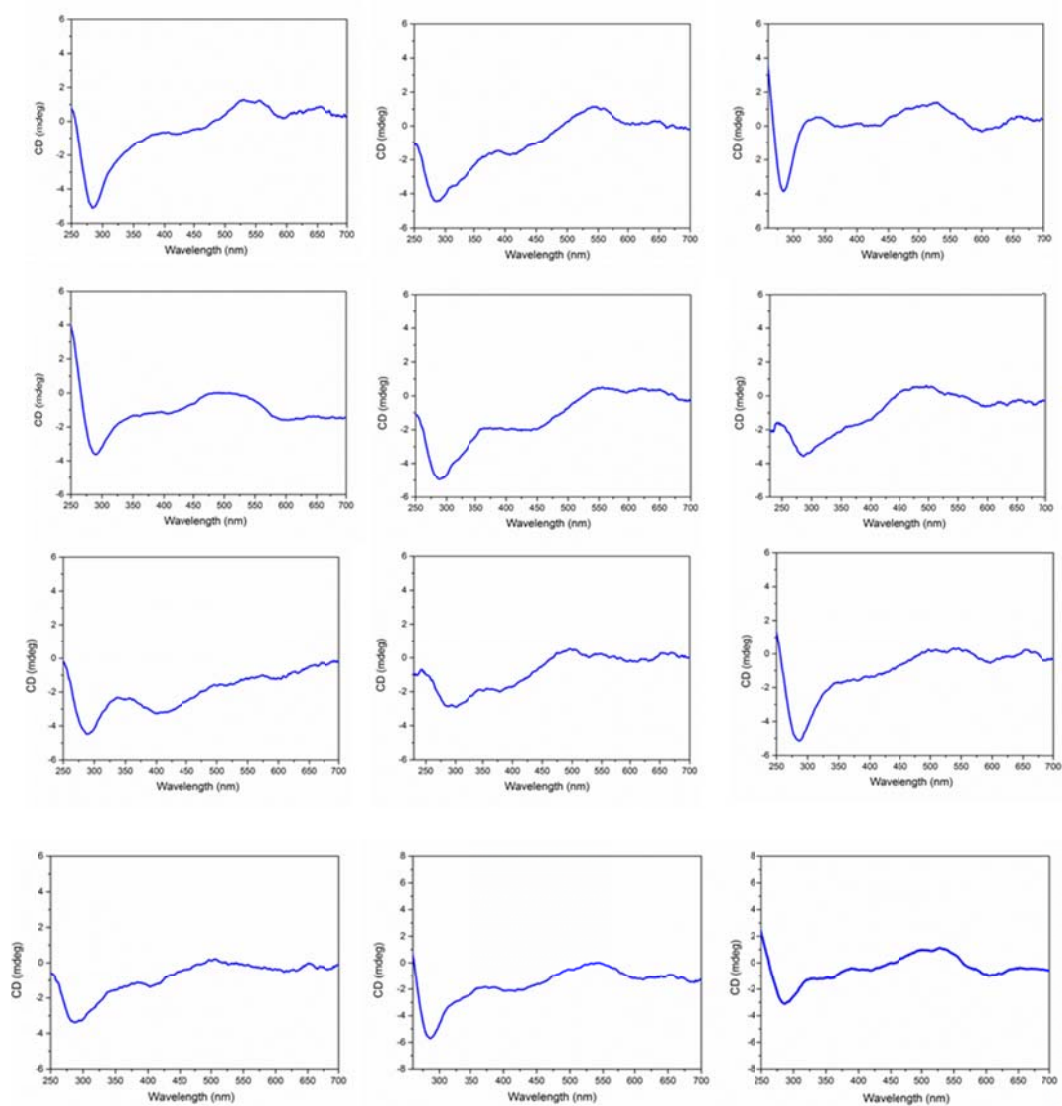


Fig. S12 Solid state CD spectra recorded for twelve blackish-purple and irregular single crystals of **1M-NH₃**. Negative dichroic signal approximately at 300 nm for all samples indicate the exclusive formation of enantiomorph **1M-NH₃**.

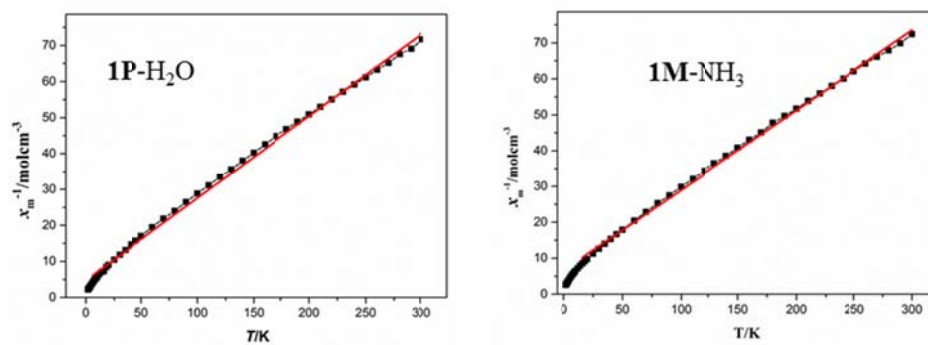


Fig. S13 Curie plot for **1P-H₂O** and **1M-NH₃**. The solid line is the best fit to the Curie-Weiss law.

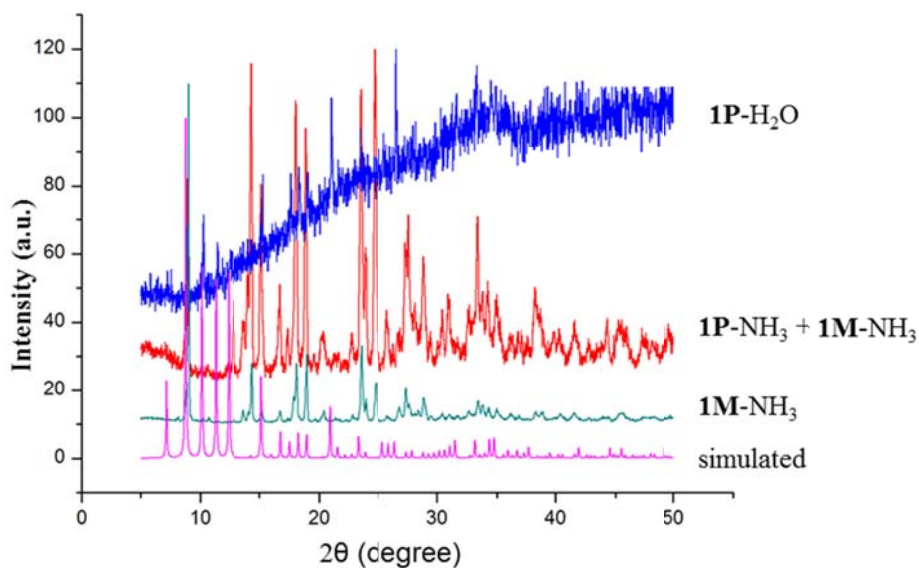


Fig. S14 Comparison of the experimental PXRD patterns of **1M-NH₃**, conglomerate **1P-NH₃ + 1M-NH₃** and **1P-H₂O** with the simulated patterns.

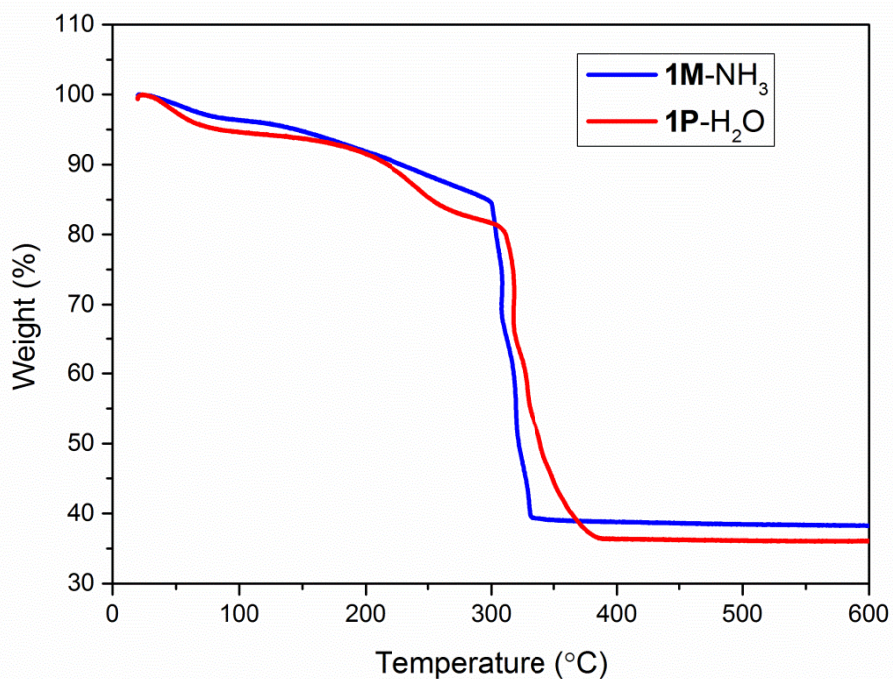


Fig. S15 TGA plots of **1P-H₂O** and **1M-NH₃** at the temperature range of 30-600 °C. The Y-axis is the percentages of residual weight.

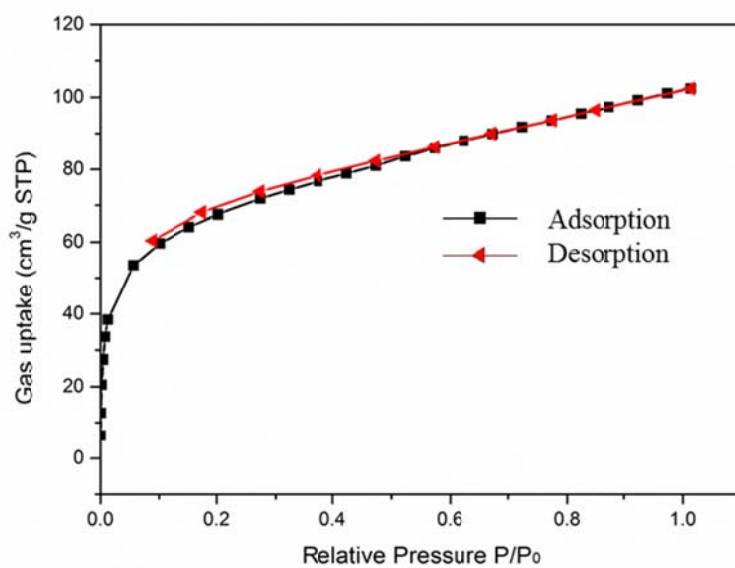


Fig. S16 CO₂ sorption isotherm of **1P-H₂O** at 195 K. P/P_0 is the ratio of gas pressure (P) to saturation pressure (P_0), with $P_0 = 1.0$ bar.

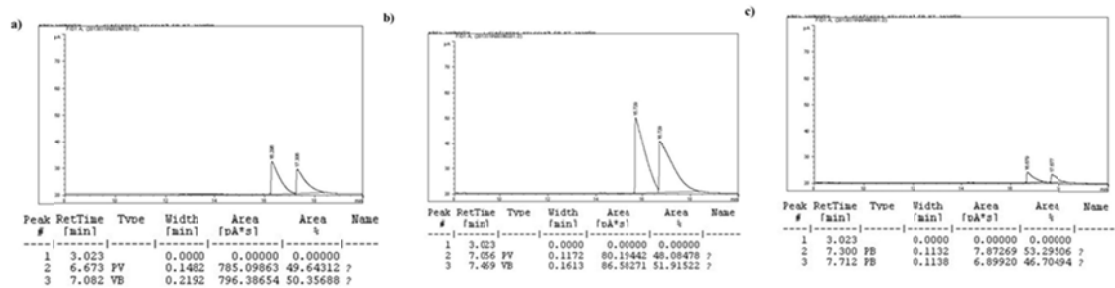


Fig. S17 Chiral GC results of the a) blank racemic 2-butanol; b) racemic 2-butanol with 1M-NH₃; c) racemic 2-butanol with 1P-H₂O.

Table S3 Chiral GC results ($ee = \frac{|(R) - (S)|}{|(R) + (S)|} \times 100\%$).

Sample	Area (%)		ee (%)
racemic 2- butanol	49.6	50.7	1.1
1M-NH ₃ + racemic 2- butanol	48.1	51.9	3.8
1P-H ₂ O + racemic 2- butanol	53.3	46.7	6.6

References:

- 1 G. M. Sheldrick, SHELXTL Reference Manual: Version 5.1, Bruker AXS, Madison, WI, **1997**.
- 2 G. M. Sheldrick, SHELXL -97: Program for Crystal Structure Refinement, University of Göttingen, Göttingen, Germany, **1997**.
- 3 A. L. Spek, *Acta Crystallogr., Sect. A*, **1990**, *46*, C34.
- 4 O. Delgado-Friedrichs and M. O' Keeffe, *Acta Crystallogr. A*, **2003**, *59*, 351. *Systre* is available at <http://www.gavrog.org/>
- 5 M. O' Keeffe, M. A. Peskov, S. J. Ramsden and O. M. Yaghi, *Acc. Chem. Res.* **2008**, *41*, 1782. RCSR is available at <http://rcsr.anu.edu.au/>